Multi-Transceiver Optical Wireless Spherical Structures for MANETs

Behrooz Nakhkoob Niasari*, Mehmet Bilgi**, Murat Yuksel**, and Mona Hella*
*Rensselaer Polytechnic Institute, ECSE Department,
110 8th Street, Troy, NY 12180, USA.
**University of Nevada - Reno, CSE Department, MS 171 1664 N. Virginia Street, Reno, NV 89557, USA.
Phone: +1 (775) 327 2246, Fax: +1 (775) 784 1877
nakhkb@rpi.edu, mbilgi@cse.unr.edu, yuksem@cse.unr.edu, hellam@ecse.rpi.edu

***Abstract*—Due to its high bandwidth spectrum, Free-Space-Optical (FSO) communication has the potential to bridge the capacity gap between backbone fiber links and mobile ad-hoc links, especially in the last-mile. Though FSO can solve the wireless capacity problem, it brings new challenges such as frequent disruption of wireless communication links (intermittent connectivity) and the line-of-sight (LOS) requirements. In this paper, we study a multi-transceiver spherical FSO structure as a basic building block for enabling optical spectrum in mobile ad-hoc networking. We outline optimal designs of such multi-transceiver subsystems such that coverage is maximized and crosstalk among neighboring transceivers is minimized. We propose a low-level packaging architecture capable of handling hundreds of transceivers on a single structure. We also present MANET transport performance over such multi-element mobile FSO structures in comparison to legacy RF-based MANETs.**

***Index Terms*—Free-Space-Optical Communication, Auto-Configurable, Angular Diversity, Spatial Reuse.**

I. Introduction

THE capacity gap between RF wireless and optical fiber backbone remains huge because of the limited availability of RF spectrum [1]. Though efforts for an all-optical Internet [2]–[7] will likely provide cost-effective solutions to the last-mile problem within the *wireline* context, high-speed Internet availability for mobile ad-hoc nodes is still mainly driven by the RF spectrum saturations, and spectral efficiency gains through innovative multi-hop techniques such as hierarchical cooperative MIMO [8]. To achieve high-speed point-to-point wireless connectivity, free-space-optical (FSO) communication has received attention particularly for high altitudes, e.g., space communications [9] and building-top metro-area communications [10], [11]. Main focus of these efforts has been on reaching *long* (i.e. ∼kms) communication distances with highly expensive (e.g., lasers) FSO components using highly sensitive mechanical steering technologies.

In commercial FSO systems, lasers in the 850nm and 1550nm band are preferred due to superior propagation characteristics in this band and higher power budget due to low geometric dispersion. Such equipment would be very costly and demands high-power in the context of multi-element scenario. Moreover, such laser-based equipment would not have the form factor, weight and power characteristics to be mounted on ad-hoc infrastructures. We instead investigate FSO systems using models of LEDs in our design as they are more amenable to dense and spatial packaging, and have longer life than lasers and fewer eye-safety regulations.

Though some preliminary multi-hop proposals exist, current FSO equipment is targeted at point-to-point links using high-powered lasers and relatively expensive components used in fiber-optical transmission. The focus of these commercial systems (e.g., Terabeam [10] & LightPointe [11]) is to form a single primary beam (and some backup beams) with limited spatial re-use/redundancy and to push the limits of transmission range, while improving link availability during poor weather conditions [12]. We instead focus on solving the LOS alignment problem with dense packaging of transceiver elements, enabling mobility through circular or spherical auto-configuring FSO systems, and target shorter per-hop distances.

Compared to radio frequency transceivers, FSO transceivers are amenable to dense integration, consume lower power, can be modulated at higher speeds, offer highly directional beams for spatial reuse/security, and operate in large swathes of unlicensed spectrum amenable to wavelength-division multiplexing (infrared/visible). To counteract these numerous advantages, optical wireless requires clear line-of-sight (LOS) between the transmitter and receiver for communication. Optical wireless communication also suffers from beam spread with distance (tradeoff between per-channel bit-rate and power) and unreliability during bad weather conditions(especially fog).

In this article, we present design considerations and studies of multi-transceiver spherical subsystems for free-space-optical mobile ad-hoc networks (FSO-MANETs). Our recent work showed that [13]–[16] FSO-MANETs can be possible by means of "optical antennas", i.e., FSO spherical structures like the one shown in Figure 1. Such FSO spherical structures (i) achieve *angular diversity* via spherical surface, (ii) achieve *spatial reuse* via directionality of FSO signals, and (iii) are *multi-element* since they are covered with multiple transceivers (e.g., LED and photo-detector pair). To avoid prohibitive costs per node, we use electronic LOS tracking and management (i.e., "*electronic steering*") methods instead of traditional *mechanical steering* techniques. For achieving ultra-high speed communications using these FSO spherical structures, high density packaging of transceivers is crucial. Thus, we focus on optimal design of multi-element FSO structures to maximize coverage and minimize crosstalk among neighboring transceivers. We also present MANET transport performance over such multi-element mobile FSO structures in comparison to legacy RF-based MANETs.

Although system parameters (e.g., divergence angle and

transmission power) can be adjusted for a specific use case, FSO especially stands out in scenarios that involve limited relative mobility of communicating nodes. Concrete examples of usage can be (as discusses in [17], [18]):

- Localized social networking applications like in a train or plane where users quickly construct an ad hoc network for information exchange purposes,
- Easier enforcement of traffic laws by enabling police cars and passenger cars to communicate in occurrence of a traffic violation. Police requests violator to slow down or stop and provide identity information for further processing and citations. No individual is required to get out of his car. Moreover, road conditions and accident information can be delivered to interested vehicles where police car and traveling cars confirm an accident and information is propagated through traffic lights and lights of other traveling cars,
- In emergency situations, emergency lights or building exit lights can communicate to victims' portable devices to inform the shortest path to a safe exit. They can also inform fire and police stations to provide more insight about the event and progress of evacuation,
- For accessibility purposes, vision or hearing-impaired person can carry a device for assistance that communicates with exit lights in buildings and traffic lights,
- Street lights and traffic lights can be used to deliver commercial content like musing and videos.

We build upon our on the idea of "spherical FSO antenna" which was proposed in [15]. The work in [15] focused on (a) presenting a toy prototype (with 4 transceivers on each side), (b) outlining a baseline LOS alignment algorithm which does not use the geometry of the spheres, and (c) finding optimal number of transceivers to place on a sphere such that the coverage is maximized. Our contributions in this article include:

- An LOS alignment and tracking algorithm which explicitly uses the geometry of the spheres (by incorporating the number of aligned transceivers into the algorithm).
- A way of designing the FSO spheres such that crosstalk among neighbor transceivers of a node is eliminated.
- A controller unit architecture which can handle hundreds of transceivers on each FSO node/antenna.
- A thorough packet-based simulation of multi-transceiver FSO nodes using realistic FSO propagation models.
- A realistic simulation model for capturing noise/interference from neighbor nodes/antennas.
- Quantification of end-to-end transport performance using our simulations of the multi-transceiver FSO systems.

The rest of the paper is organized as follows: We start with investigating optimal design and packaging issues of multi-transceiver FSO spheres in Section II. We outline how characteristics of these spherical designs can be used for LOS detection and maintenance as well as consider feasibility of digital controller architecture capable of handling such highly dense packaging of FSO transceivers. Then, in Section IV, we present a simulation study of transport performance over our FSO spherical structures with a focus on the intermittency of the mobile wireless links among these structures. Finally, we summarize our work in Section V.

II. Physical Layer Design Considerations for Multi-Channel Mobile FSO Communication

Despite its huge potential benefits, FSO communication suffers from high sensitivity to adverse weather conditions and line-of-sight (LOS) requirements. Extensive research has been done to overcome adverse weather effects on the quality of transmission [19] [20] [21]. But for LOS detection, it has mostly been addressed for communication between static nodes or those with low mobility using opto-electro-mechanical beam steerers [22] [23], and silicon imagers [24] [25]. To our knowledge, none of published research has addressed the design of multi-channel communication between mobile transceivers (a.k.a. transmitter-receiver pairs) while addressing cross-talk issues and electronic LOS detection.

For a multi-channel optical communication receiver, highly integrated photo-detector (PD) arrays are required to interface with high speed amplifiers. The speed of amplifiers for optical communications has been reported up to 10xGbps [26] [27] [28]. However, the integration of massive arrays of PDs with the amplifiers is still a subject of active research [29] [30]. The design of the physical layer for the case of multi-channel optical communication under mobile scenarios (airplanes, cars, etc.) is even more complicated due to the continuous LOS detection requirement and crosstalk elimination. This would require a controller unit in both the transmitter and receiver with operating speed exceeding that of the individual communication links. The operation of one transceiver's controller unit has to be synchronized with other controller units, i.e., the controller units have to employ specific PDs in the receiver array and LEDs in the transmitter array for an active wireless link. Further, the receiver side needs to determine the corresponding coverage area and maintain its allocation with the movement of the transmitter side. If the parallel links carry different data, the digital controller in the receiver side must be aware of the crosstalk areas and accordingly ignore the output of the PDs in that area. Thus, the controller has to determine which PD is in the coverage area of which transmitter. Addressing all these constraints is almost impossible for a linear array. Thus, we have recently proposed an omni-directional *optical antenna* [15] formed of a spherical structure tessellated with equally spaced hexagons of transceiver units as shown in Figure 1.

Based on the spherical optical antenna concept, we develop a mathematical algorithm for detection and establishment of LOS between the optical elements of such antennas. We use this mathematical algorithm to design a digital controller for controlling the elements of the arrays both in the receive and transmit sides. Additionally, we calculate the pitch between two adjacent transmitters required to eliminate any crosstalk between their emitted optical signals. Thus, the area which is illuminated by every single transmitter on the surface of spherical antenna in the receiver side can be exactly determined. The outlined control mechanism will allow electronic LOS detection and maintenance while eliminating the possibility of cross-talk between multiple optical links without using any mechanical devices like gimbals or mirrors.

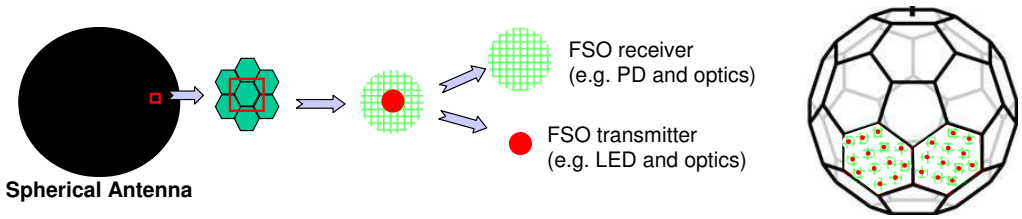

Fig. 1. Spherical optical antenna tessellated with PDs and LEDs/laser diodes.

A. Calculation of the Number of Communicating Optical Elements

Consider two spherical optical antennas of the type depicted in Figure 1, one acting as a transmitter and the other as a receiver. Assume *d* is the distance between the centers of the communicating spherical antennas. To use the spherical antenna for multi-channel communication, we need to estimate the number of LEDs/laser diodes in the transmitter and the corresponding number of illuminated PDs on the receiver side. The first glance at Figure 2 gives the impression that half of the transmitter side surface is in LOS with half the surface of the receiver side. However, the diodes on the surface of the transmitter are emitting their optical signals around an axis between the focal point of the transmitting sphere and the center of every diode, with a divergence angle that takes a conical shape. On the other hand, every PD, has a field of view which will determine the angle between the detectable optical beam arriving on it and the axis between its center and the focal point of the receiver sphere similar to the transmitter case (Figure 2(a)). Based on this, we can estimate the areas on the surface of the transmitter and receiver when they are in LOS as shown in Figure 2(b).

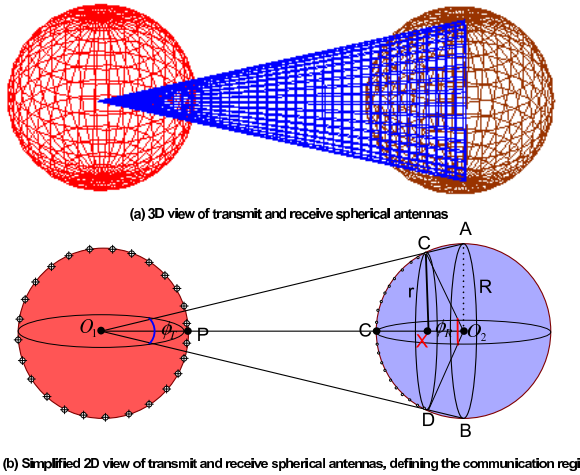

Fig. 2. Calculation of the number of PDs on the surface of the receiver which are in LOS with the LEDs/laser diodes on the surface of the transmitter.

Assume N_R is the total number of the PDs on the receiver sphere, N_T is the total number of LEDs on the transmitter surface, and n_r is number of the illuminated photodetectors. Also, assume that the two spheres are identical, each with a radius R. In the following equations, we will estimate the distance between the transmitter and the receiver *d* as well as their communication angles ϕ_T and ϕ_R as in Figure 2(b). The formulas can also be easily extended to unequal transmit and receive antennas. In Figure 2, the illuminated surface on the receiver side can be given as

$$S_R = 4\pi R^2 \frac{n_r}{N_R} \tag{1}$$

The communication angle on the receiver side equals

$$\phi_R = 2\pi \frac{n_r}{N_R} \tag{2}$$

while the radius of the circle facing the illuminated PDs in the received area equals

$$r = Rsin\frac{\phi_R}{2} \tag{3}$$

Further, the distance *d* between the two centers O_1 and O_2 can be calculated as follows

$$\frac{r}{R} = \frac{O_1X}{O_1O_2} = \frac{d - O_2X}{d};\ \ O_2X = \sqrt{R^2 - r^2};$$
$$\Rightarrow d = R\sqrt{\frac{R+r}{R-r}} = R\sqrt{\frac{1+sin\pi\frac{n_r}{N_R}}{1-sin\pi\frac{n_r}{N_R}}} \tag{4}$$

where $d \geq 2R$.

Based on (1) to (4), we can calculate the corresponding parameters in the transmitter side

$$\phi_T = 2\arctan\sqrt{\frac{1-sin\pi\frac{n_r}{N_R}}{1+sin\pi\frac{n_r}{N_R}}} \tag{5}$$

The active surface on the transmitter which is in LOS with S_R according to 1 is given by S_T, where

$$S_T = 2\phi_T R^2 \tag{6}$$

Thus, the number of LEDs on the surface of the transmitter which are in LOS with n_r PDs on the receiver's surface is given by n_t

$$n_t = N_T \frac{arctan\sqrt{\frac{1-sin\pi\frac{n_r}{N_R}}{1+sin\pi\frac{n_r}{N_R}}}}{\pi} = N_T(\frac{1}{4} - \frac{n_r}{2N_R}) \tag{7}$$

where N_T is total number of the LEDs on the surface of transmitter. Interestingly, (7) is a linear function,which would simplify the design of the controller unit, and speed up the tracking algorithm. Figure 3 plots equations (4), (5), and (7) and shows the normalized distance between the centers of two spheres $\frac{d}{R}$, the transmission angle ϕ_T, and the percentage of LEDs on the surface of the transmitter $\frac{n_t}{N_T}$ versus the number of illuminated photo diodes with respect to the total number of PDs $\frac{n_r}{N_R}$. For practical considerations, the communication

between the two spherical antennas is only valid when the distance between their centers is equal or higher than $2R$; i.e. the two spheres are not touching. This results in an $\frac{n_r}{N_R}$ ratio higher than $.2048$, according to (4). The ultimate value for $\frac{n_r}{N_R}$ is obviously 0.5, which corresponds to the case of the two spheres infinitely far from each other.

From Figure 3, we can easily see that at $d = 2R$. In other words, when the two spheres are tangential to each other, the transmission angle ϕ_T is 53.13^o which corresponds to 14.77% percent of the LEDs/laser diodes in the transmitter that can be in LOS with the PDs on the receiver side. As the distance between the communication nodes increases, the transmission angle will decrease, indicating a lower number of LEDs that can be used for communications. As the distance goes to infinity, the number n_T, falls to 1 which means that only one LED can be communicating with half of the receiver sphere.

B. Crosstalk Elimination in Multi-channel FSO Communication

For reliable and secure multi-channel FSO communication link, we need to study the crosstalk resulting from the overlap between the emitted rays of different elements in the array architectures. In the spherical architecture, there is a minimum angle between the center of every two adjacent transmitter elements, below which crosstalk will occur. This angle can be *conservatively* estimated as the angle at which the two rays $L1$ and $L2$ in Figure 4 are in parallel, assuming divergent optical beams.

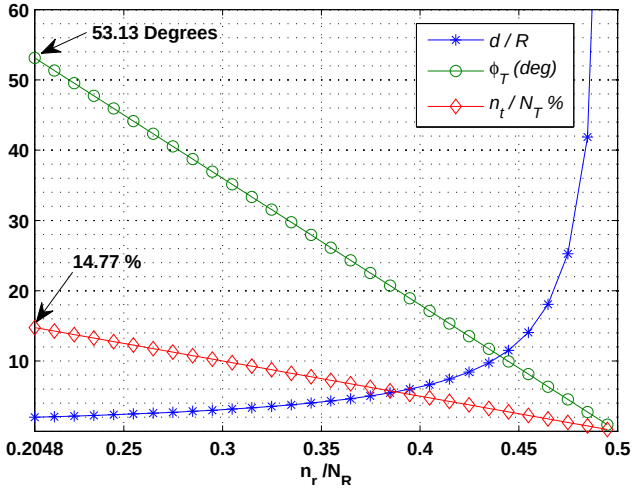

Fig. 3. Graph of normalized distance, transmission angle, and percentage of transmitter elements, versus the normalized number of illuminated receiver elements

From Figure 4(b), we can calculate ϕ_0 at which the two rays $L1$ and $L2$ are in parallel. It can be verified that this condition is simply :

$$\phi_0 = \phi_d \tag{8}$$

where ϕ_d is the divergence angle of every LED.

For parallel multi-channel FSO communication link without crosstalk between adjacent communicating channels, a pitch angle equal to the divergence angle would enable a coverage pattern around the transmitter sphere as shown in Figure 5.

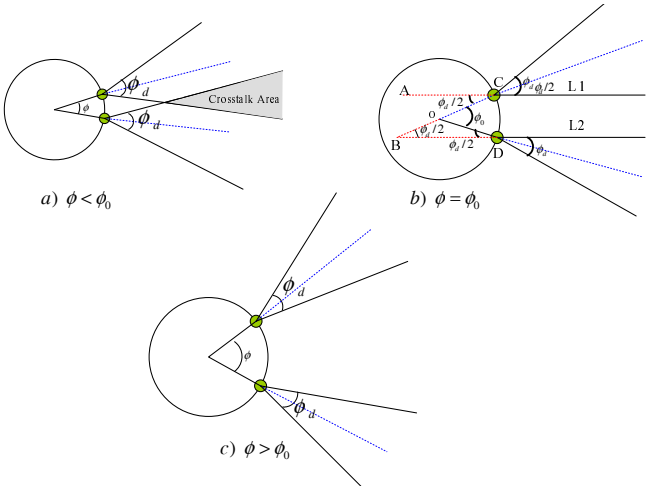

Fig. 4. Illustration of the effect of the pitch between adjacent transmitters on the crosstalk in multi-channel optical communication

As can be seen, on the receiver surface there are two completely separated areas from two different transmitter elements ($Area1$ and $Area2$). This spatial guard range is analogous to the case of a guard band between the frequency spectrums of adjacent communication channels in RF communication. In the case of using spherical antennas for optical communications, one can use a guard area between the two adjacent optical coverage areas on the receiver surface to eliminate the possibility of crosstalk. The proposed guard area has several advantages when considering practical implementation issues. First, by introducing the guard band, we are eliminating the possibility of injection of the photo-generated charge carriers from illuminated photo diodes in the coverage area of one LED to the coverage area of another LED, and vice versa. Second, it simplifies the design of the controller responsible for determining the number and exact position of PDs which are in the coverage area of each channel, as will be explained further in the following section. It is worth noting that the above discussion focuses on cross-talk between two neighboring spheres. For multiple communicating nodes, eliminating cross-talk would require resource allocation similar to RF communication by assigning different time, wave length, or code.

C. Architecture of The Controller Unit

The function of the controller unit is to establish and maintain LOS for various channels under mobility conditions. This requires understanding the sequence of events/procedures that have to take place between the two communicating nodes as shown in Figure 6.

First, the transmitting sphere emits a pilot signal from all of its transmitting elements in all directions (i.e., the spherical transmitter acts as an omni-directional optical antenna). On the other side, the controller of the spherical antenna in the receive mode will sequentially monitor the outputs of all of its receiving elements. Each receive element in the receiver side consists of a PD followed by an amplifier and a buffer stage. In addition, each node has a flag indicating that it has received a pilot signal and is in LOS with a transmitter somewhere. Moreover, every node on the surface of the antenna will

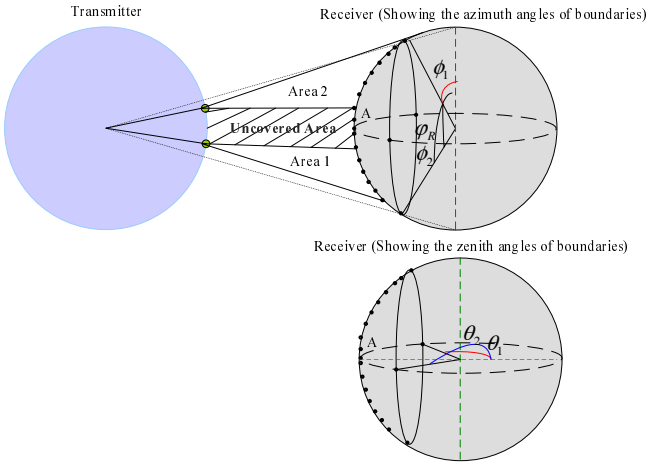

Fig. 5. Illustration of multi-channel communication link showing two possible coverage areas or two channels with a guard-range for cross talk elimination

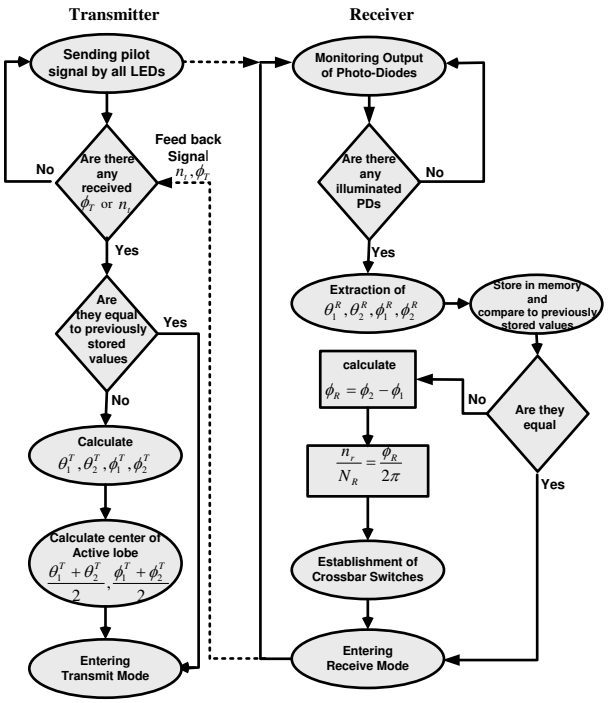

Fig. 6. Sequence of events in the transmitter and receiver to track LOS, and secure communication.

have one byte for its azimuth angle, and one for its zenith, to uniquely define its position in spherical coordinates. The numbers specifying the position of every element on the surface are fixed and will not change during motion or rotation. The digital controller repeatedly sweeps the output of all the nodes and just saves the azimuth and zenith angles of the edges of the illuminated lobe at the end of every cycle (θ_1, θ_2, ϕ_1, ϕ_2 in Figure 5). Rather than following the sequence of calculation from (1) to (7), the controller will initially calculate ϕ_R, as $\phi_2 - \phi_1$ in Figure 5. The use of ϕ_R will enable the calculation of an approximate value for the number of illuminated PDs

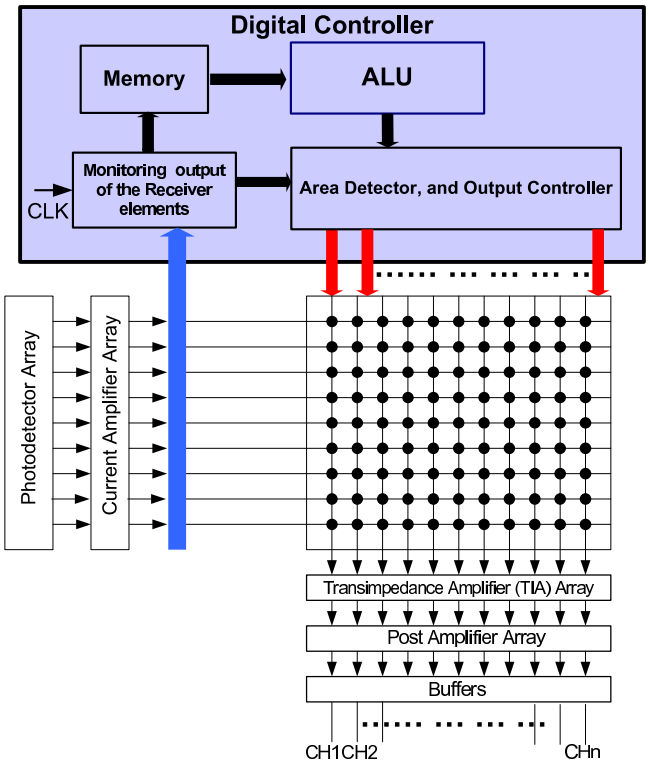

Fig. 7. Block Diagram of the whole FSO optical Receiver

n_r which is overestimated due to ignoring the guard area. After the calculation of ϕ_R, the digital controller will follow the calculations in (2) to (7). Now, the receiver must send a feedback signal to the transmitter to acknowledge that there are some receiver elements in LOS with the transmitter. This feedback signal will consist of ϕ_T and n_t, according to (5) and (7). However, on the transmit side, the transmit controller needs to locate the exact position of the angle ϕ_T on the surface which can be determined by knowing the center of the active surface on the transmitter side, S_T. This point can be illuminated on the surface of the transmitter by sending the feedback signal using the center element on the receiver side. Note that both receiver and transmitter have arrays of receivers and transmitters as depicted in Figure 1. Thus, we need to distinguish the center point in the receiver side (Point A in Figure 5). This can be done, simply using the coordinates of this point, which are ($\frac{\phi_2+\phi_1}{2}$) and ($\frac{\theta_2+\theta_1}{2}$). The process of finding the center is repeated by the digital controller of the transmitter to specify the center point of the active area S_T on the transmitter side. Knowing this point and ϕ_T, the transmitter is able to specify the active area, which is in LOS with the receiver. If the pitch angle between the transmitter elements, in the transmitter side, is equal or more than divergence angle, we can use all the transmitters in the specified region without any crosstalk. As the formulas for establishing this locking or synchronization condition are simple enough, the digital controller can calculate them rapidly and issue the feedback signal to the transmitter, at a higher rate than the speed of the mobile communicating nodes. Note that the feedback signal from the receiver can also be a simple RF signal that can be

TABLE I
TABLE OF DEFAULT VALUES COMMON TO EACH SIMULATION SET IN OUR EXPERIMENTS.

Parameter Name	Default Value
Number of nodes	49
Number of flows	49x48
Visibility	6 km
Number of interfaces	8
Mobility	1 m/s
Simulation time	3000 s
Transmission range and separation between nodes	30 m
Area	210 m by 210 m
Node radius	20 cm
Divergence angle	0.5 rad
Photo detector diameter	5 cm
LED diameter	0.5 cm

used as an acknowledge signal to transmitter, indicating that LOS is maintained.

In order to determine the PDs that will be assigned to receive signals from each individual channel, referring to Figure 5, the digital controller can use the boundaries of the guard area. In other words, the coverage area in the receiver side consists of different well defined separated areas. Using this property, the digital controller simply assigns these separate illuminated areas to different transmitters.

For the detection of the signal from each transmitting element, a crossbar switch architecture can be used as shown in Figure 7. The crossbar switch is inserted between typical optical communication circuit blocks formed of an input low noise amplifier that is directly connected to the PD array, while the output of the switches go to additional amplifier stages that convert the current input to voltage output (transimpedance amplifier TIA). The voltage signals are supplied to a limiting amplifier array and output buffers followed by data and clock recovery circuitry. The details of each circuit block is beyond the scope of this article.

The digital controller also has a monitoring block, which searches for pilot signals, followed by memory, Arithmetic logic unit (ALU), and controller unit for ON/OFF controlling of the crossbar switches to estimate the number of active parallel channels and related PDs for every coverage area as shown in (1) to (7), and previous sections.

III. SIMULATION OF MULTI-ELEMENT SPHERICAL FSO STRUCTURES

To obtain a better understanding of how our proposed multi-element spherical FSO node designs would perform, we develop simulation modules for these designs and experiment with various scenarios. It is especially not possible to analytically model complex situations that can happen in a mobile setting involving many spherical FSO structures. In our simulations, we consider a packet-based communication environment while accounting for additional protocol overheads for (i) LOS alignment detection and maintenance, and (ii) handoff among transceiver elements.

NS-2 [31] is a well-recognized platform for network research. This platform has served as a basic tool for simulation of networks with acceptable closeness to reality. NS-2 has also received attention as a modifiable platform as it is possible to introduce new modules and derivatives of existing objects since it is an open source implementation. Hence, we implemented a set of NS-2 components to simulate networks of multi-element FSO ad-hoc nodes. Our contribution to NS-2 package includes:

- Directional FSO antenna model with 3-D pointing and divergence angle features, as well as necessary fields to represent accompanied LED/transmitter and photo-detector components.
- A mechanism for periodic establishment of alignment lists for each transceiver for uni-directional and bi-directional scenarios.
- A new alignment-table based channel model for delivering packets only to the candidate receiver antennas that reside in the transmitter's alignment list.
- FSO power calculator to calculate the necessary source power to transmit a packet of known size to a target at given range, and under provided parameters such as visibility in the medium, receive threshold, transmitter and receiver diameters, divergence angle, desired error probability per bit and noise.
- Calculation of received power based on Gaussian-distributed geometric beam spread and orientation of receiving photo-detector (Figure 10(a).
- Calculation of noise heard in the medium during transmission of a packet (Figure 10(b)).
- FSO modulation mechanism to calculate error probability for given received power, visibility in the medium, separation of transmitter and receiver, atmospheric attenuation and heard noise during transmission.
- Simple obstacle simulation mechanism for recognizing nodes as obstacles at the same time to avoid beams getting through nodes.
- Stamping of each transmitted and received packed with the direction information of the used antenna using an extra packet header field.

Such FSO extensions to NS-2 enabled us to run simulations that can provide insightful information about the scaling behavior of FSO networks in terms of throughput as well as effects of individual system parameters on the per-flow throughput.

A. Alignment Lists and Alignment Timer

We implemented a timer mechanism in NS-2 that goes off every half-a-second and determines the available alignments among the transceivers. The timer mechanism has an identical counterpart in the design of the multi-element FSO node structure as described in Section II-C. This *auto-alignment* [32] process involves a search phase and a data phase. The search phase looks for available alignments from the neighboring structures while the data phase sends the data on the aligned transceivers.

An ongoing transmission may experience a disconnection due to mobility of either structures. In such a disconnection, auto-alignment circuitry is designed to start a *search phase*. The search phase results in possible alignment establishments whereas the timer will do the same in a simulation scenario.

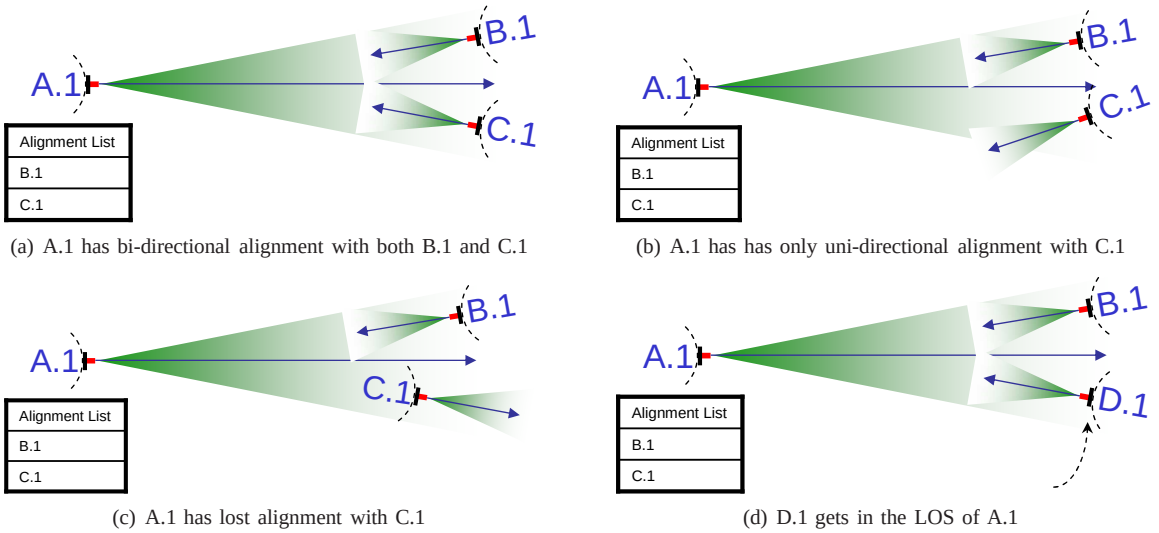

(a) A.1 has bi-directional alignment with both B.1 and C.1

(b) A.1 has has only uni-directional alignment with C.1

(c) A.1 has lost alignment with C.1

(d) D.1 gets in the LOS of A.1

Fig. 8. Types of possible alignment loss/gain during a timer period.

We argue that 0.5 second is a long enough period for alignment detection and establishment, especially for scenarios in which high mobility is involved. Hence, the mutual alignment between two transceivers might not be preserved. We depict the possible events that can occur before the timer goes off in a scenario with multiple transceivers each from different nodes (A, B, C and D). In the simplest case, alignments can stay unmodified like in Figure 8(a).

In Figure 8(b), we see that node C moved and its transceiver C.1 can not see transceiver A.1 anymore. But, transceiver A.1 can still see C.1 and because the timer is not fired yet, A.1 continues to keep an entry for C.1 in its alignment list. Notice that, if the timer expires in such a case, C.1 will not be placed in A.1's list since the alignment in between the two is not mutual, i.e., both A.1 and C.1 should see each other.

Note that this is a conservative assumption for LOS establishment and there is still room for improvement. In this case where only uni-directional alignment is available, transceiver A.1 will be able to send packets to C.1, but C.1 will not be able to reach A.1 in our implementation.

For the third case, C.1 might have turned its back or just moved out of line-of-sight of A.1. Hence both have lost alignment with each other and although they will continue to keep entries for each other until the alignment timer expires, packets will be dropped.

The fourth case is; a new transceiver, D.1, gets in the LOS of A.1. Another major conservative assumption is; regardless of alignment's nature, uni-directional or bi-directional, D.1 will not receive any of the packets that A.1 sends and vice versa. If D.1 stays in LOS of A.1, new entries will be created for each other in their alignment lists during the next search phase.

Once the alignment timer expires, it takes one primary transceiver at a time and creates a list of candidate transceivers that both the primary transceiver and candidate transceiver are in each others' line-of-sight, hence the term "mutual alignment". The nodes in current simulations are assumed to be in 2 dimensional flat space. However, since the normal of an antenna is represented in 3 dimensions, it is easily achievable to simulate spherical FSO nodes placed in 3 dimensional space.

B. FSO Node Structure Design Internals

The default wireless node implementation in NS-2 is illustrated in Figure 9(a). We modified this internal structure to meet our needs by changing AODV to make it capable of handling multiple link layers. From the perspective of IP, AODV routing protocol handles multiple transceivers and considers them as separate network interfaces. Hence, each transceiver has a separate stack with 802.11 Wireless MAC, interface queue and a link layer object along with an alignment list in NS-2 terms as illustrated in Figure 9(b).

In our current design, considering that each transceiver has its own stack and a list of aligned interfaces, whenever AODV chooses to send a packet through an interface, the customized channel implementation will deliver the packet to each transceiver that is stored in the senders alignment list. This delivery process will take the alignment loss cases in Figure 8 into account as discussed earlier.

In our current implementation (Figure 9(b)), when the alignment timer expires, new alignment lists are established for each transceiver. From the AODV's point-of-view, each entry in the alignment list corresponds to a link. Note that whenever we change the alignment lists, we are not notifying AODV explicitly to indicate some of the links are down. Hence, AODV itself discovers which of the previously established links are down and also the newly available links. This discovery may take up to multiples of the used "hello" interval for links that went down and one "hello" interval for new neighbors. Thus, in the design depicted in Figure 9(b), neither the routing protocol can handle neighbor changes in a timely manner, nor reducing alignment interval would yield to increased responsiveness.

IV. Transport Performance over Multi-Element FSO Nodes

Our proposition for new mobile FSO structures is backed by rigorous simulation of various scenarios. These simula-

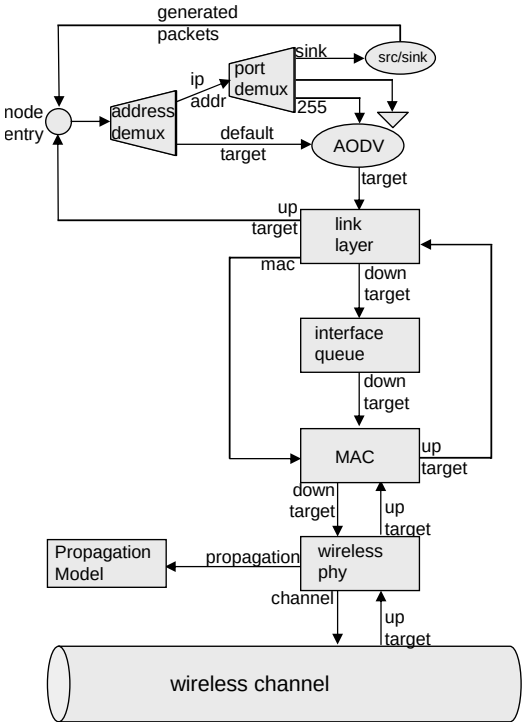

(a) Structure of a wireless node in NS-2. Note that AODV routing protocol can handle only one network interface by default.

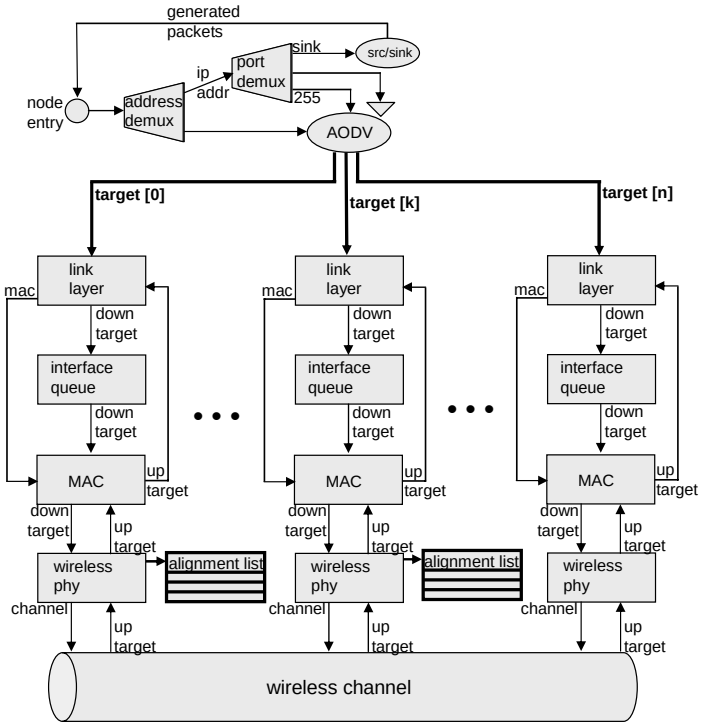

(b) FSO node structure with a separate stack for each optical transceiver. AODV is modified so that it is capable of handling multiple network interfaces. WirelessPhy is also modified to keep a list of aligned transceivers. (Link layers' up-target reference is omitted for clarity.)

Fig. 9. Multi-transceiver wireless node designs in NS-2.

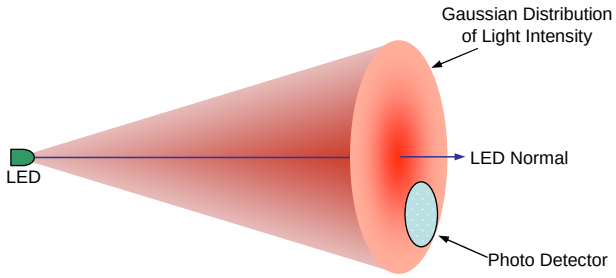

(a) Gaussian distribution of light intensity at the receiver plane.

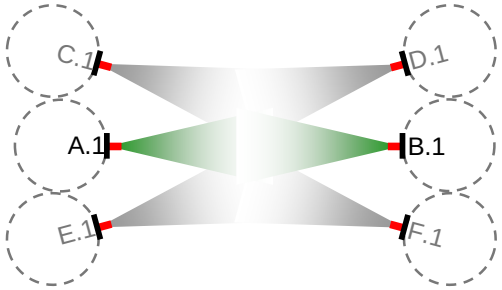

(b) Noise in FSO transmission: transceivers C.1, D.1, E.1 and F.1 contribute to the noise for the communication between A.1 and B.1.

Fig. 10. Noise and Gaussian light intensity of FSO beam.

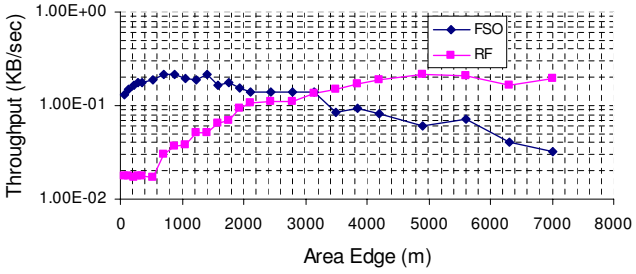

(a) RF and FSO converge to a common throughput when the transmission power is adjusted accordingly. Later on, RF performs better than FSO for larger areas.

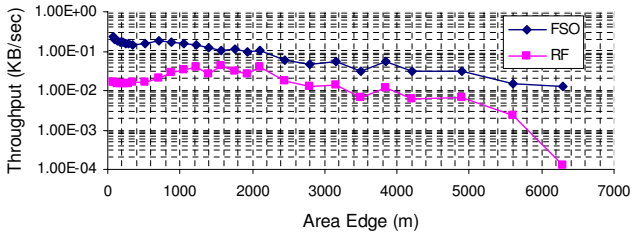

(b) Throughput drops dramatically for both FSO and RF when the simulation area is expanded but the transmission power is kept the same.

Fig. 11. Node density in the network.

tions allow us to observe the potential effects of our multi-transceiver spherical FSO structures on the upper layers of the protocol stack. Due to the sensitive nature of optical wireless communication, the wireless links among our spherical structures exhibit an intermittently connected behavior depending on various parameters such as mobility speed and transmit/receive angle of transceiver units. It is especially well-known that TCP's end-to-end performance might degrade significantly due to such fragile intermediate wireless links, which we investigate through simulations.

We designed each simulation scenario to identify the effect of one particular system parameter. We used a 7x7 perfect node grid with 30 meters of separation between neighboring nodes. In this 49-node network with 6 km of medium visibility, each node establishes FTP sessions to every other node that lasts 3000 seconds, creating 49x48 many FTP sessions. Nodes preserve their locations in stationary simulations and typical speed parameter for mobile simulations is 0.1 meter/sec (from Table I).

To make our simulations realistic, we revised the NS-2 implementation of a wireless channel. We used well-known FSO propagation models [33] to simulate power attenuation characteristics of an FSO signal, optimistically considering only a non-turbulent propagation medium. LEDs' light intensity profile follows the Lambertian law [33], i.e., intensity is directly proportional to the cosine of the angle from which it is viewed. Also, the light intensity is modeled by Gaussian distribution to determine the density of the illumination based on the distance of PD from LED's normal. We accounted for both the atmospheric attenuation and the geometric spread in our FSO propagation simulations [16]. Our noise calculation assumes that there are beams that are not delivered by the channel object in NS-2 because of used alignment list mechanism. Hence, when we need to calculate the noise affecting a reception, we go through all the transmissions coming from neighbor nodes at that moment and determine their contribution to the noise by using the mentioned power calculation process.

In order to make a fair comparison of RF and FSO performance, we assign RF reception power threshold and FSO source power such that the RF and FSO nodes successfully reach to the same distance with a BER of 10^{-6}. There are 8 interfaces each with a divergence angle of .5 rad (corresponding to a medium-to-low quality LED), placed on a circular node with 20cm radius. Diameter of transmitter LED is 0.5cm and the diameter of receiver PD is 5 cm.

First of the simulation scenarios adjusts the transmission power of both FSO and RF while expanding the simulation area (Figure 11(a)). The transmission power is adjusted such that each node can establish 10^{-6} BER communication links to its immediate neighbor, regardless of the distance between the nodes. This means that RF nodes will have to spend significantly more transmission power to keep their BER at 10^{-6}. In this scenario, simulation area is changed from 70m x 70m to 7km x 7km. For scenarios in which the area edge is less than 2km, FSO performs better than RF. They converge to a common throughput at 2km and RF starts to perform better than FSO after this point. This is due to the fact that there

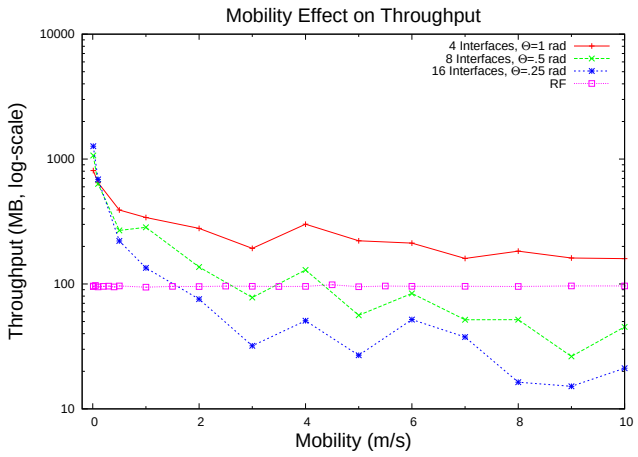

Fig. 12. Effect of increased mobility on FSO and RF.

are more uncovered areas in the case of FSO. Though we are not showing the power consumption results, RF spends a lot more power to maintain the communication links to immediate neighbors. So, FSO is still performing better in terms of throughput per power. In the fixed power scenario (Figure 11(b)), both FSO and RF performance drop severely since the power is not adjusted accordingly.

We investigated the effect of mobility on FSO networks and compared it with RF (Figure 12). We found that increased mobility poses the challenge of intermittent connectivity, i.e., because the underlying physical link experiences frequent disconnections, per-node TCP throughput performance degrades dramatically. Moreover, as we increase speed of each node in the network towards 10 m/s, the difference in physical link availability for RF and FSO becomes more distinguishable; RF performance follows a nearly stable profile. We conclude that, to achieve high throughput performance even in highly mobile networks, we need to reconsider design decisions of higher layers in the TCP/IP stack; by refactoring to a more disconnection tolerant design by introducing buffers and use of directional MAC. Buffers at multiple layers and directional MAC will be holding packets at the event of link failure (i.e., misalignment of interfaces) with the optimism that the link will be up soon. Because NS-2's random waypoint algorithm is used to determine the nodes' routes while roaming, we argue that it is highly likely to obtain better throughput results in mobile cases such as vehicular and naval networks since relative mobility of nodes to each other is small.

Our third simulation set attempts to conclude on the divergence angle of transceivers (Figure 13). In this set, we construct nodes with different number of transceivers. As we increase the divergence angle for each of the setups from 0.1 rad to 1 rad, the general trend of overall network throughput is towards decreasing. We conclude that since the divergence angle is the reason for spatial overlap between neighboring transceivers on a node, as the field of view of a transceiver gets wider, we start to see crosstalk. This crosstalk increases the noise if it does not cause interference. Hence, the network experiences a worse throughput.

Lastly, our visibility results (Figure 14) are obtained using

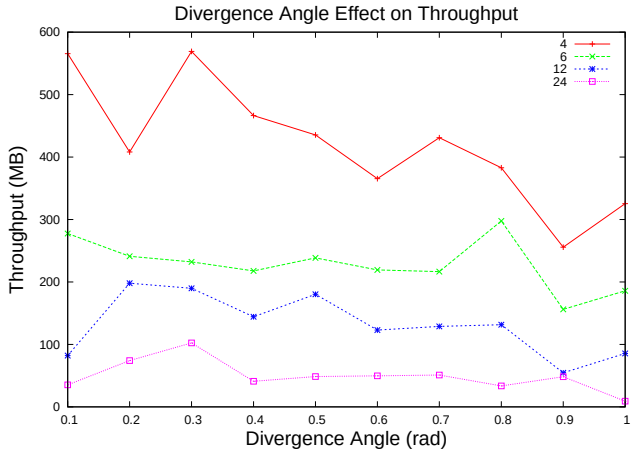

Fig. 13. Effect of divergence angle on throughput.

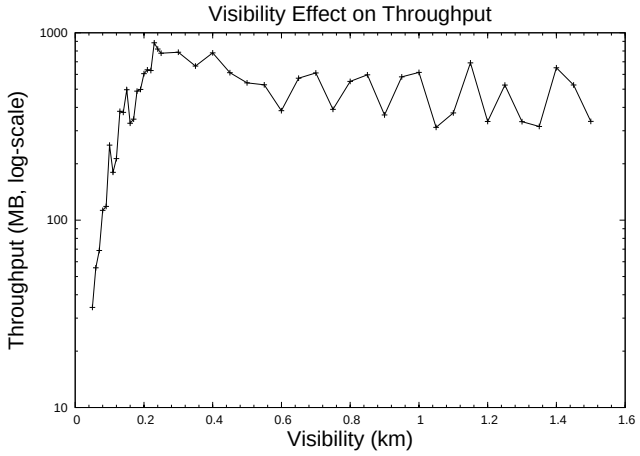

Fig. 14. Effect of increased medium visibility on FSO throughput. Transmission power is adjusted for 0.5 km visibility and 10^{-6} noise.

the typical mobile setup. We fix the transmission power using the parameters in Table I, except the visibility. While calculating power, we set visibility to 0.5 km. In our simulations, we start with 0.05 km and increase it up to 1.5 km. We see that the network throughput increases dramatically as we have better visibility in the medium. This is due to the decreased error probability for each packet that is caused by the atmospheric attenuation of the light.

V. Summary and Discussions

Compared to radio frequency communications, free-space-optical (FSO) communication offers many advantages including a widely available and unlicensed frequency spectrum, low transmission power, secure communication, and low cost installation. Despite these inherit benefits, FSO suffers from high sensitivity to adverse weather condition and line of sight requirements. In this paper, we presented the novel concept of spherical optical antenna for electronic line-of-sight detection and multi-channel optical communication. We addressed the design of the physical layer responsible for LOS establishment and maintenance and crosstalk elimination in parallel multi-channel communication between highly portable objects. To the best of our knowledge, this is the first design concept that relies totally on electronic rather than mechanical techniques to address optical wireless communications between portable or mobile nodes. The design of the proposed digital controller within the physical layer enables the calculation of the number of transmit/receive pairs that are in LOS at specific time and/or position, and accordingly the assignment of multiple communication channels to different transmit/receive pairs with sufficient guard range for cross-talk elimination. The digital controller maintains the synchronization between the mobile communicating nodes at all times to prevent the loss of data. Existing nanometer technologies allow the design of optical transceivers front-end circuits as well as digital controllers in the range of Gigabits per second. Thus, the response of the proposed physical layer in the detection of relative movement between transmitter and receiver would potentially be much higher than speed of mobile communicating nodes.

Future work includes prototype implementation of the presented multi-element spherical structures in a MANET setting. Such structures can be useful for illumination purposes if visible optoelectronic transmitters are used.

Acknowledgment

This work is supported in part by NSF under awards 0721452 and 0721612.

References

[1] Christopher Davis and Zygmunt Haas and Stuart Milner, "On How To Circumvent The Manet Scalability Curse," in *Proceedings of IEEE MILCOM*, 2006.
[2] "Toward an all-optical Internet," Lightwave, November 1998.
[3] M. Yoo and C. Qiao and S. Dixit, "Optical burst switching for service differentiation in the next-generation optical Internet," *IEEE Communications Magazine*, vol. 39, no. 2, pp. 98–104, 2001.
[4] R. Ramaswami and K. N. Sivarajan, *Optical networks: A practical perspective*, Morgan Kaufmann Series In Networking, 1998.
[5] C. Qiao and M. Yoo, "Optical burst switching (OBS): A new paradigm for an optical Internet," *Journal of High Speed Networks*, vol. 8, no. 1, pp. 69–84, 1999.
[6] A. R. Moral and P. Bonenfant and M. Krishnaswamy, "The optical Internet: architectures and protocols for the globalinfrastructure of tomorrow," *IEEE Communications Magazine*, vol. 39, no. 7, pp. 152–159, 2001.
[7] D. K. Hunter and I. Andonovic, "Approaches to optical Internet packet switching," *IEEE Communications Magazine*, vol. 38, no. 9, pp. 116–122, 2000.
[8] A. Ozgur and O. Leveque and D. Tse, "Hierarchical Cooperation Achieves Optimal Capacity Scaling in Ad Hoc Networks," submitted to IEEE Transactions on Information Theory, 2006, http://arxiv.org/PS_cache/cs/pdf/0611/0611070.pdf.
[9] V. W. S. Chan, "Optical space communications: a key building block for wide area space networks," *IEEE Lasers and Electro-Optics Society*, vol. 1, pp. 41–42, 1999.
[10] "Terabeam Inc.," 2004, http://www.terabeam.com/.
[11] "Lightpointe Inc.," 2004, http://www.lightpointe.com/.
[12] G. Pang et al., "Optical Wireless based on High Brightness Visible LEDs," in *IEEE Industry Applications Conference*, 1999, vol. 3, pp. 1693–1699.
[13] J. Akella, C. Liu, D. Partyka, M. Yuksel, S. Kalyanaraman, and P. Dutta, "Building blocks for mobile free-space-optical networks," *Proceedings of IFIP/IEEE International Conference on Wireless and Optical Communications Networks (WOCN)*, pp. 164–168, Mar 2005.
[14] J. Akella, M. Yuksel, and S. Kalyanaraman, "Error analysis of multi-hop free-space-optical communication," *Proceedings of IEEE International Conference on Communications (ICC)*, vol. 3, pp. 1777–1781, May 2005.
[15] M. Yuksel, J. Akella, S. Kalyanaraman, and P. Dutta, "Free-Space-Optical Mobile Ad Hoc Networks: Auto-Configurable Building Blocks," Wireless Networks (in press), 2009.

[16] M. Bilgi and M. Yuksel, "Multi-Element Free-Space-Optical Spherical Structures with Intermittent Connectivity Patterns," in *Proceedings of IEEE Infocom Student Workshop*, 2008.
[17] "IEEE P802.15.7 Task Group Visible Light Communication," http://www.ieee802.org/15/pub/TG7.html.
[18] "Visible Light Communications Consortium," http://www.vlcc.net.
[19] S. Arnon, "Effects of atmospheric turbulence and building sway on optical wireless-communication systems," *SPIE Optics Letters*, vol. 28, no. 2, pp. 129–131, January 2003.
[20] Z. Jia, Q. Zhu and F.A O, "Atmospheric attenuation analysis in the FSO link," *International Conference on Communication Technology*, pp. 1–4, November 2006.
[21] M. Aharonovich and S. Arnon, "Performance improvement of optical wireless communication through fog with a decision feedback equalizer," *Journal of Optical society of America*, vol. 22, no. 8, pp. 1646–1654, August 2005.
[22] M. Last, B. S. Leibowitz, B. Cagdaser, A. Jog, L. Zhou, B. E. Boser and K. Pister, "Toward a wireless optical communication link between two small unmanned aerial vehicles," in *Proceeding of International Symposium on Circuits And Systems*, 2003, vol. 3, pp. 930–933.
[23] A. Portillo, G. G. Ortiz, and C. Racho, "Fine Pointing control for optical communications," in *IEEE Proceeding of Aerospace conference* , March 2001, vol. 3, pp. 1541–1550.
[24] B. Leibowitz, B. Boser, and K. Pister, "A 256-Element CMOS imaging receiver for Free-Space optical communication," *IEEE Journal of Solid State Circuits*, vol. 40, no. 9, pp. 1948– 1956, September 2005.
[25] V. M. Joyner, D. M. Holburn, D. C. O'Brien, and G. E. Faulkner , "A CMOS Imaging Diversity Receiver Chip with a Flip-Chip Imaging detector Array for optical wireless links," *IEEE Lasers and Electro-Optics*, pp. 927–928, October 2006.
[26] C. Kromer, G. Sialm, T. Morf, M.L. Schmatz, F. Ellinger, D. Erni., and H. Jackel, "A Low power 20 GHZ, 52 db ohm, transimpedance amplifier in 80 nm CMOS," *IEEE Journal of Solid State Circuits*, vol. 39, no. 6, pp. 885–894, June 2004.
[27] C. Chan and O. Chen, "A 10 Gb/sec CMOS Optical Receiver using modified regulated cascode scheme," in *Proc. of IEEE Mid West Symposium on Circuits and Systems*, August 2005.
[28] S. Palermo, A. Emami-Neyestanak, and M. Horowitz, "A 90 nm CMOS 16Gb/s Transceiver for optical interconnects," *International Solid State Circuits Conference, Dig. of Tech. papers*, pp. 44–46, February 2007.
[29] H. Sharifi and S. Mohammadi, "Heterogeneously Integrated 10Gb/s CMOS optoelectronic receiver for long haul telecommunication," *IEEE Radio Frequency Integrated Circuits*, pp. 515–518, June 2007.
[30] M. Jutzi, M. Grozing, E. Gaugler, W. Mazioschek, and M. Berroth , "2 Gb/s CMOS optical integrated receiver with a spatially modulated photodetector," *IEEE photonic technology letters*, vol. 17, no. 6, pp. 1268–1270, June 2005.
[31] "Network Simulator 2," http://isi.edu/nsnam/ns/.
[32] M. Yuksel, J. Akella, S. Kalyanaraman, and P. Dutta, "Free-Space-Optical Mobile Ad Hoc Networks: Auto-Configurable Building Blocks," Wireless Networks (in press), 2008.
[33] H. Willebrand and B. S. Ghuman, *Free Space Optics*, Sams Pubs, 2001, 1st Edition.

Behrooz Nakhkoob received B.S. and M.Sc. degrees both in Electrical engineering from IUST (Iran Univ. of Sci. & Tech.) Tehran in 1994 and 1997 respectively. From 1997 to 2000, he was with research department of IRIB (National broadcasting Center of Iran), in which he developed professional analog video Teletext Encoder system for the first time in Iran. From 2000 to 2008, he was with Electronic and instrumentation department of NRI (Niroo Research Institute, Tehran-Iran). In Jan.2009, he joined the Department of Electrical and System Engineering of Rensselaer Polytechnic Institute in Troy, NY, as a Ph.D. student, working on integrated circuit design for high data rate wireless optical receivers. His interests lie in high frequency and high speed analog circuit design for wireless and wireline applications.

Mehmet Bilgi is a Ph.D. student at the CSE Department of The University of Nevada - Reno (UNR) and he is working under supervision of Dr. Yuksel. His current research focuses on several aspects of multi-element free-space-optical mobile ad-hoc networks including throughput analysis and comparison, prototyping, localization and buffering. His research interests are in computer networks area. He received his M.S. degree from UNR in 2008 and B.S. degree from Computer Engineering Department of Fatih University, Istanbul, Turkey in 2005. He is a member of IEEE.

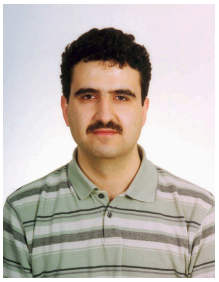

Murat Yuksel is currently an Assistant Professor at the CSE Department of The University of Nevada - Reno (UNR), Reno, NV. He was with the ECSE Department of Rensselaer Polytechnic Institute (RPI), Troy, NY as a Postdoctoral Research Associate and a member of Adjunct Faculty until 2006. He received a B.S. degree from Computer Engineering Department of Ege University, Izmir, Turkey in 1996. He received M.S. and Ph.D. degrees from Computer Science Department of RPI in 1999 and 2002 respectively. His research interests are in the area of computer communication networks with a focus on protocol design, network economics, wireless routing, free-space-optical mobile ad-hoc networks (FSO-MANETs), and peer-to-peer. He is a member of IEEE, ACM, Sigma Xi, and ASEE.

Mona Hella received B.Sc. and and M.S. degrees with Honors from Ain-Shams University, Cairo, Egypt, in 1993 and 1996 respectively, and Ph.D. degree, in 2001, from The Ohio State University, Columbus, Ohio, all in Electrical Engineering. From 1993 to 1997, she was a teaching and research assistant at Ain Shams University. From 1997-2001, she was a research assistant at the Ohio State University, working on RF circuits for wireless applications. She was with the Helsinki university of Technology (HUT), Espoo, Finland as a visiting scholar in 1998, and with the analog group at Intel cooperation, Chandler, AZ in Summer 1999. She was a senior designer at Spirea AB, Stockholm, Sweden working on CMOS power amplifiers (2000-2001). From 2001 to 2003, she was a senior designer at RFMD Inc, Billerica, MA working on Optical communication systems, as well as silicon-based wireless systems. She joined the Electrical, Computer and Systems Engineering department at Rensselaer Polytechnic Institute as an Assistant Professor in 2004. Her research interests include the areas of mixed-signal and radio frequency IC design for wireless and wire-line applications.